Proceedings of the ASME 2009 International Design Engineering Technical Conferences & Computers and Information in Engineering Conference
IDETC/CIE 2009
August 30 - September 2, 2009, San Diego, California, USA

DETC2009-87081

OPTIMAL CONTROL FOR A PITCHER'S MOTION MODELED AS CONSTRAINED MECHANICAL SYSTEM

Sina Ober-Blöbaum*
Control and Dynamical Systems
California Institute of Technology
Pasadena, CA 91125
sinaob@cds.caltech.edu

Julia Timmermann
Heinz Nixdorf Institute, Control Engineering and Mechatronics
University of Paderborn
D-33098 Paderborn, Germany
julia.timmermann@rtm.upb.de

ABSTRACT

In this contribution, a recently developed optimal control method for constrained mechanical systems is applied to determine optimal motions and muscle force evolutions for a pitcher's arm. The method is based on a discrete constrained version of the Lagrange-d'Alembert principle leading to structure preserving time-stepping equations. A reduction technique is used to derive the nonlinear equality constraints for the minimization of a given objective function. Different multi-body models for the pitcher's arm are investigated and compared with respect to the motion itself, the control effort, the pitch velocity, and the pitch duration time. In particular, the use of a muscle model allows for an identification of limits on the maximal forces that ensure more realistic optimal pitch motions.

INTRODUCTION

The computation of optimal motion sequences of biomechanical multi-body systems is of great interest in many different research areas, especially the optimal control of the motion of the human body itself. For several reasons it is important to understand the muscle activation and coordination, e.g. to construct prothesis and implants in modern medical surgery.

As a first step in that direction, in this work we use a recently developed method, namely Discrete Mechanics and Optimal Control for Constrained Systems (DMOCC [1]) to determine the optimal motion of a pitcher's arm that allows him to maximize the velocity of his pitch. In extension to previous work in [1,2] we also take the interaction of the muscles into account. This leads on the one hand to more insight into the optimal time evolution of the muscle forces acting in the joints, on the other hand the muscle model automatically provides bounds on the maximal producible forces leading to a more realistic model.

Optimal Control for Constrained Mechanical Systems

DMOC (Discrete Mechanics and Optimal Control, [2,3]) is a local optimal control method developed for mechanical systems. It is based on the discretization of the variational structure of the mechanical system directly in contrast to other methods like, e.g. shooting, multiple shooting, or collocation methods. These methods rely on a direct integration of the associated ordinary differential equations (see e.g. [4–7]). In the context of variational integrators (see [8]), the discretization of the Lagrange-d'Alembert principle leads to structure (symplectic-momentum) preserving time-stepping equations. These serve as equality constraints for the resulting finite dimensional nonlinear optimization problem that can be solved by standard nonlinear optimization techniques like sequential quadratic programming (SQP, see e.g. [9, 10]). The extension to constrained mechancial systems (DMOCC) was developed in [1, 11]. Within the constrained formulation, the system is described in terms of redundant coordinates subject to holonomic constraints. For multi-body systems, the couplings between the bodies are characterized by holonomic constraints describing the kinematic conditions arising from the specific joint connections. These configuration constraints are

*Address all correspondence to this author.

enforced using Lagrange multipliers within the discrete variational principle. However, the presence of the Lagrange multipliers in the set of unknowns enlarges the number of equations. To reduce the number of unknowns (configurations and torques at the time nodes) and thereby the dimension of the discrete system, the discrete null space method in conjunction with a nodal reparametrization in generalized coordinates is used. This method was introduced in [12] for the simulation of multi-body systems without control.

This procedure on the one hand leads to lower computational cost for the optimization algorithm and on the other hand inherits the conservation properties from the constrained scheme. The benefit of exact constraint fulfillment, correct computation of the change in momentum maps and good energy behavior is guaranteed by the resulting optimization algorithm as shown in [1]. In particular, these are important benefits for the optimal control of high dimensional rigid body systems with joint constraints.

The Pitch Model

In this article, we apply the developed method to the optimization of a pitch motion. The simplified model we investigate was already introduced in [1] and [2]. The kinematic chain representing the pitcher's arm consists of three parts: the collarbone, the upper and the forearm. The goal is to maximize the final velocity of the forearm's center of mass in pitch direction. For the model in [1] and [2] it is assumed that a motion of the multi-body system is induced by external control torques that act in the joints. However, the realistic simulation and optimization of human motion cannot be done without the modeling of muscles. They not only make active body motion possible, but also constrain the maximal producible muscle forces, what is important for the simulation of realistic motions. Maximal and minimal values for the muscle forces are difficult to measure in reality. Rather than defining artificial bounds on the external control torques to constrain the producible muscle force, the use of a configuration- and velocity-dependent muscle function provides realistic bounds in a natural way dependent on the angle and the angular velocity between two limbs.

The different aspects of the muscle model we use for the optimization was initially introduced in [13–16]. The length dependency of the muscle force was analyzed by Murray et al. [14] by a study of cadavers. The relation between the contraction velocity and the muscle force is a common model that was introduced by Hill [15]. To determine the external muscle force, geometry functions are required that were derived in [13] and [16] for different muscles. These are the basic principles of a simplified muscle model. The authors of [17] use these basic principles in a new model and investigate the stability properties of the elbow with a load. The main aim is to demonstrate that stable equilibrium states exist just on grounds of the mechanical properties of the muscle and the skeleton. We enhance parts of this model to generate a muscle model that is suitable for the simulation of the pitch motion.

This Contribution

In this work we investigate three different multi-body models for the pitcher's arm that are characterized by different joint couplings and control parameters. Firstly, we introduce the formulation and the solution method DMOCC for the optimal control of constrained mechanical systems. Secondly, we present the different joint connections and the resulting constraints on the system. Besides the use of joints that have been introduced in [1,12] within the framework of the discrete nullspace method, a new hinge joint is presented. Thirdly, the muscle model used for one of the multi-body models is described in detail. To obtain realistic motions, constraints on the joint angles and torques are indispensible. These are formulated as additional constraints on the optimization variables. The goal of the optimization is to maximize the final velocity of the forearm's center of mass in pitch direction while the pitch time is an additional free variable. The use of many initial guesses leads to different results for each model. These solutions are analyzed with respect to the motion itself, the control effort, the objective function value, and the pitch duration time. Finally, we give further ideas for future steps for the optimization in biomechanics and sports.

OPTIMAL CONTROL FOR CONSTRAINED MECHANICAL SYSTEMS

Consider an n-dimensional mechanical system with time-dependent configuration vector $q(t) \in Q$ and velocity vector $\dot{q}(t) \in T_{q(t)}Q$, where $t \in [0,T]$. Let the configuration space be constrained by the function $g(q) = 0 \in \mathbb{R}^m$ which defines the submanifold on configuration Q and tangent space TQ as $\mathcal{C} = \{q \,|\, g(q) = 0\} \subset Q$ and $T\mathcal{C} = \{(q,\dot{q}) \,|\, g(q) = 0,\ \nabla g(q) \cdot \dot{q} = 0\} \subset TQ$, respectively. The constrained mechanical system has to be moved along a configuration curve $q(t) \in \mathcal{C}$ during the time interval $t \in [0,T]$ from an initial state $(q^0, \dot{q}^0) \in T\mathcal{C}$ to a final state $(q^T, \dot{q}^T) \in T\mathcal{C}$ under the influence of a force $f : Q \times U \to T^*Q$, where $T^*_{q(t)}Q$ is the dual space of $T_{q(t)}Q$. This force depends on a time dependent control parameter $u(t) \in U$ that influences the motion of the system. Due to the presence of constraints, the forces f are not independent. They can be expressed in terms of the control parameter dependent generalized forces $\tau(u(t)) \in W \subseteq R^{n-m}$.

The curves q and u are to be chosen to minimize a given objective functional $J : TQ \times U \to \mathbb{R}$

$$J(q,\dot{q},u) = \int_0^T C(q(t),\dot{q}(t),u(t))\,dt \tag{1}$$

with the cost function $C : TQ \times U \to \mathbb{R}$, such that the motion

has to be in accordance with the equation of motion of the constrained mechanical system. These are desribed via a constrained version of the Lagrange-d'Alembert principle requiring

$$\delta \int_0^T \left(L(q,\dot{q}) - g^T(q)\lambda\right) dt + \int_0^T f \cdot \delta q \, dt = 0 \qquad (2)$$

for all variations $\delta q \in TQ$ and $\delta\lambda \in \mathbb{R}^m$ vanishing at the endpoints with the time dependent Lagrange multipliers $\lambda(t) \in \mathbb{R}^m$. The Lagrangian $L : TQ \to \mathbb{R}$ consists of the difference of the kinetic energy $\frac{1}{2}\dot{q}^T M\dot{q}$ with the mass matrix $M \in \mathbb{R}^{n,n}$ and the potential energy function $V : Q \to \mathbb{R}$. The constrained Lagrange-d'Alembert principle (2) leads to the differential-algebraic system of equations of motion

$$\frac{\partial L(q,\dot{q})}{\partial q} - \frac{d}{dt}\left(\frac{\partial L(q,\dot{q})}{\partial \dot{q}}\right) - G^T(q)\lambda + f = 0, \qquad (3a)$$

$$g(q) = 0, \qquad (3b)$$

where $G(q) = \nabla g(q)$ denotes the Jacobian of the constraints. The vector $G^T(q)\lambda$ represents the constraint force that prevents the system from deviations off the constraint manifold $\mathcal{C}$.

DISCRETE MECHANICS AND OPTIMAL CONTROL FOR CONSTRAINED SYSTEMS

The optimal control problem stated in Eqn. (1) and Eqn. (3) in combination with desired boundary constraints is now transformed into a finite dimensional constrained optimization problem by using a global discretization of the states and controls.

Discrete Mechanics and Optimal Control

We replace the state space TQ by $Q \times Q$ (which is locally isomorphic to TQ) and consider the grid $\Delta t = \{t_k = kh \,|\, k = 0,\ldots,N\}$, $Nh = T$, where N is a positive integer and h the step size. We replace the paths $q : [0,T] \to Q$ and $\lambda : [0,T] \to \mathbb{R}^m$ by discrete paths $q_d : \{t_k\}_{k=0}^N \to Q$ and $\lambda_d : \{t_k\}_{k=0}^N \to \mathbb{R}^m$, where we view $q_k = q_d(kh)$ and $\lambda_k = \lambda_d(kh)$ as an approximation to $q(kh)$ and $\lambda(kh)$, respectively (see [2, 3, 8]). Similarly, we replace the control path $u : [0,T] \to U$ by a discrete one. To this end, we consider a refined grid $\Delta\tilde{t}$, generated via a set of control points $0 \le c_1 < \cdots < c_s \le 1$ as $\Delta\tilde{t} = \{t_{k\ell} = t_k + c_\ell h \,|\, k = 0,\ldots,N-1; \ell = 1,\ldots,s\}$. With this notation, the discrete control path is defined to be $u_d : \Delta\tilde{t} \to U$. We define the intermediate control samples u_k on $[t_k, t_{k+1}]$ as $u_k = (u_{k1},\ldots,u_{ks}) \in U^s$ to be the values of the control guiding the system from $q_k = q_d(t_k)$ to $q_{k+1} = q_d(t_{k+1})$, where $u_{kl} = u_d(t_{kl})$ for $l \in \{1,\ldots,s\}$.

We approximate the action integral in Eqn. (2) by a discrete Lagrangian $L_d : Q \times Q \to \mathbb{R}$,

$$L_d(q_k, q_{k-1}) - \frac{1}{2}g_d^T(q_k)\lambda_k - \frac{1}{2}g_d^T(q_{k+1})\lambda_{k+1} \qquad (4a)$$

$$\approx \int_{kh}^{(k+1)h} \left(L(q(t),\dot{q}(t)) - g^T(q)\lambda\right) dt \qquad (4b)$$

and discrete forces

$$f_k^- \cdot \delta q_k + f_k^+ \cdot \delta q_{k-1} \approx \int_{kh}^{(k+1)h} f \cdot \delta q(t)\, dt,$$

where f_k^+, f_k^- are the left and right discrete forces, respectively. They are specified in Eqn. (10). The discrete version (5) of the constrained Lagrange-d'Alembert principle (2) requires the discrete path $\{q_k\}_{k=0}^N$ and multipliers $\{\lambda_k\}_{k=0}^N$ to satisfy

$$\begin{aligned}\delta \sum_{k=0}^{N-1} & L_d(q_k, q_{k+1}) - \tfrac{1}{2}g_d^T(q_k)\lambda_k - \tfrac{1}{2}g_d^T(q_{k+1})\lambda_{k+1} \\ & + \sum_{k=0}^{N-1} \left(f_k^- \cdot q_k + f_k^+ \cdot \delta q_{k+1}\right) = 0\end{aligned} \qquad (5)$$

for all variations $\{\delta q_k\}_{k=0}^N$ and $\{\delta\lambda_k\}_{k=0}^N$ with $\delta q_0 = \delta q_N = 0$ and $\delta\lambda_0 = \delta\lambda_N = 0$, which is equivalent to the constrained forced discrete Euler-Lagrange equations

$$D_2 L_d(q_{k-1}, q_k) + D_1 L_d(q_k, q_{k+1}) - G_d^T(q_k)\lambda_k + f_{k-1}^+ + f_k^- = 0, \qquad (6a)$$

$$g_d(q_{k+1}) = 0, \qquad (6b)$$

for $k = 1,\ldots,N-1$ where $G_d(q_k)$ denotes the Jacobian of $g_d(q_k)$. In the same way, we obtain via an approximation of the objective functional (1), discrete objective functions C_d and J_d, respectively as

$$J_d(q_d, u_d) = \sum_{k=0}^{N-1} C_d(q_k, q_{k+1}, u_k). \qquad (7)$$

The problem of minimizing the discrete objective function (7) subject to the forced discrete Euler-Lagrange equations (6) and boundary conditions results in a nonlinear optimization problem with equality constraints, which can be solved by standard optimization methods like SQP. Optionally, we can also include inequality constraints on states and controls.

System Reduction

To reduce the number of equations and variables in the system stated in Eqn. (6), we make use of the discrete null space method introduced in [12]. Assuming that the constraints are independent, for every $q_k \in \mathcal{C}$, the basis vectors of $T_{q_k}\mathcal{C}$ form an $n \times (n-m)$ null space matrix $P(q_k)$ with corresponding map $P(q_k) : \mathbb{R}^{n-m} \to T\mathcal{C}$ with

$$\text{range}(P(q_k)) = \text{null}(G(q_k)) = T_{q_k}\mathcal{Q}. \tag{8}$$

Thus, premultiplication of Eqn. (6a-b) by $P^T(q_k)$ eliminates the discrete constraint forces including the discrete Lagrange multipliers from the system. Furthermore, we can reduce the system to the minimal possible dimension by a reparametrization of the constraint manifold $\mathcal{C}$ and the force manifold $T^*\mathcal{Q}$. At the time nodes, q_k is expressed in terms of the discrete generalized coordinates $\theta_k \in \Theta \subseteq R^{n-m}$ as

$$R_d : \Theta \subseteq \mathbb{R}^{n-m} \times \mathcal{Q} \to \mathcal{C},\ q_k = R_d(\theta_k, q_{k-1}), \tag{9}$$

such that the constraints $g(q_k) = g(R_d(\theta_k, q_{k-1})) = 0$ are satisfied. The dependent components of the discrete force vectors f_{k-1}^+ and f_k^- can be calculated by using the left and right discrete generalized forces $\tau_{k-1}^+, \tau_k^- \in W \subseteq \mathbb{R}^{n-m}$

$$f_{k-1}^+ = B^T(q_k)\tau_{k-1}^+ \text{ and } f_k^- = B^T(q_k)\tau_k^-, \tag{10}$$

where the matrix $B(q_k) : W \to T^*\mathcal{Q}$ depends on the specific joint connections and constraints $g(q_k)$.

Remark For our problem we use an absolute reparametrization $q_k = R_d(\theta_k, q_{00})$, where $q_{00} \in \mathcal{C}$ is a fixed reference configuration, relative to which the initial configuration is computed and θ_k describes the change in the variable θ from time t_0 to t_k. This is in contrast to the relative reparametrization defined in Eqn. (9), where θ_k constitutes the change of θ in the time interval $[t_k, t_{k+1}]$. The formulation with an absolute reparametrization provides computational efficiency and an easier construction of initial guesses for the optimal control problem, while the reparametrization is still unique due to appropriate constraints on the discrete generalized coordinates θ_k.

Approximation

Balancing accuracy and efficiency, we approximate the discrete objective function C_d and the discrete Lagrangian L_d with the midpoint rule as

$$C_d(q_k, q_{k+1}, u_k) = hC\left(\frac{q_{k+1}+q_k}{2}, \frac{q_{k+1}-q_k}{2}, u_k\right), \tag{11}$$

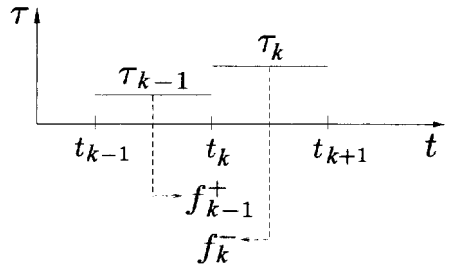

Figure 1. RELATION OF REDUNDANT FORCES AT t_k TO PIECEWISE CONSTANT DISCRETE GENERALIZED FORCES.

$$L_d(q_k, q_{k+1}) = hL\left(\frac{q_{k+1}+q_k}{2}, \frac{q_{k+1}-q_k}{h}\right). \tag{12}$$

The control parameters are assumed to be constant in each time interval, i.e. $l = 1$ and $c_1 = \frac{1}{2}$. Thus, if the discrete generalized forces themselves play the role of controls, their effect acting in $[t_{k-1}, t_k]$ and in $[t_k, t_{k+1}]$ is transformed to the time node t_k via

$$\tau_{k-1}^+ = \frac{h}{2}\tau_{k-1} \text{ and } \tau_k^- = \frac{h}{2}\tau_k, \tag{13}$$

where $\tau_k = u_k$ (cf. Fig. 1). In the case where the generalized forces depend on the generalized configurations and velocities, we again employ the midpoint rule for the approximation

$$\tau_{k-1}^+ = \frac{h}{2}\tau\left(\frac{\theta_k+\theta_{k-1}}{2}, \frac{\theta_k-\theta_{k-1}}{h}, u_{k-1}\right), \tag{14}$$

$$\tau_k^- = \frac{h}{2}\tau\left(\frac{\theta_{k+1}+\theta_k}{2}, \frac{\theta_{k+1}-\theta_k}{h}, u_k\right), \tag{15}$$

with u_k being the control parameter. The constraints and multipliers are evaluated at the time nodes themselves as

$$g_d^T(q_{k+1})\lambda_{k+1} = hg^T(q_{k+1})\lambda_{k+1}. \tag{16}$$

Constrained Optimization Problem

The overall problem is to find discrete generalized quantities $\theta_d = \{\theta\}_{k=0}^N$, $u_d = \{u\}_{k=0}^{N-1}$ that minimize the discrete objective function (7) subject to the reduced system given in minimal dimension

$$P^T(q_k)\left(D_2L_d(q_{k-1}, q_k) + D_1L_d(q_k, q_{k+1}) + f_{k-1}^+ + f_k^-\right) = 0 \tag{17}$$

and subject to boundary conditions. Here, q_k and $f_k^\pm$ are given by Eqn. (9) and Eqn. (10), respectively.

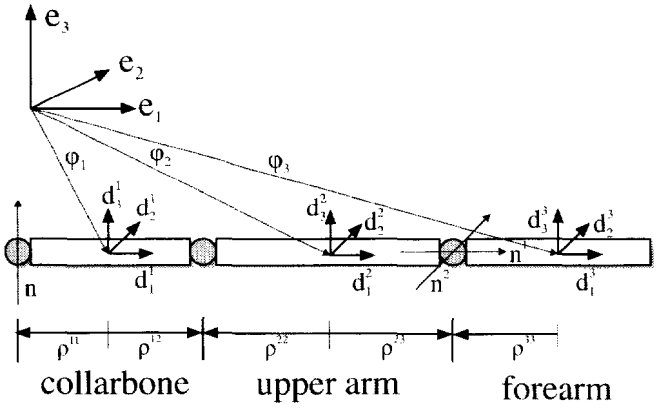

Figure 2. MODEL OF THE PITCHER'S ARM CONSISTING OF COLLARBONE, UPPER ARM, AND FOREARM.

MODEL OF PITCHER'S ARM

To optimize the pitcher's motion we consider a kinematic chain representing the arm including the collarbone, the upper and the forearm (cf. Fig. 2). The single rigid bodies are interconnected by joints (J_i) and are moved via torques $\tau^{(J_i)}$, $i = 1,2,3$, that act in the joints. In this article, we investigate three different multi-body models for the arm. These are characterized by the use of different joints and control magnitudes. We will first briefly summarize the rigid body formulation introduced in [12]. Secondly, we give a detailed description for all joints and controls in use as well as the resulting constraints on the system. Expressions for the null space matrices and the reparametrizations have been derived in [12] and [18]. A description of the redundant forces is given in [1] and [18].

Rigid Body Formulation

The placement of a material point in the body's configuration $X = X_I d_I \subset \mathbb{R}^3$ relative to an orthonormal basis $\{e_I\}$ fixed in space can be described as

$$x(X,t) = \varphi(t) + X_I d_I(t), \tag{18}$$

where $X_I \in \mathbb{R}$, $I = 1,2,3$, represent coordinates in the body-fixed director triad d_I (cf. Fig. 2). The configuration variable of a rigid body $q(t) = (\varphi(t), d_1(t), d_2(t), d_3(t)) \in \mathbb{R}^{12}$ is described via the placement of the center of mass $\varphi \in \mathbb{R}^3$ and the directors $d_I \in \mathbb{R}^3, I = 1,2,3$. The body's rigidity assumption, that the directors are constraint to be orthonormal during the motion, leads to six independent constraints as $\frac{1}{2}(d_I^T \cdot d_I) = 1, I = 1,2,3$, and $d_I^T \cdot d_J = 0$ for $I,J \in \{1,2,3\}, I < J$.

Kinematic joints

Two adjacent rigid bodies are connected via a kinematic joint (J). In the following description, the configuration vector q consists of all rigid body coordinates, q^i, $i = 1,2,3$, where the motion of the i-th body relative to the $(i-1)$-th body is restricted via the constraints $g^{(J_i)}$. The spherical joint (S_2) prevents relative translations between the collarbone and the upper arm such that only a three-dimesional rotational motion $\theta^{(S_1)} \in \mathbb{R}^3$ is allowed. Thus, the constraints on the system are given as

$$g^{(S_2)}(q) = \varphi^2 - \varphi^1 + \rho^{22} - \rho^{12} = 0 \in \mathbb{R}^3,$$

where ρ^{ij}, $i,j = 1,2$ is the vector from the i-th body's center of mass to the j-th joint in body-fixed frame. In addition, the revolute joint (R_3) allows the forearm to rotate only around the axis n^2 that is fixed in the upper arm. This leads to five constraints as

$$g^{(R_3)}(q) = \begin{pmatrix} \varphi^3 - \varphi^2 + \rho^{33} - \rho^{23} \\ (n^2)^T \cdot d_I^3 - \eta_I, I = 1,2 \end{pmatrix} = 0 \in \mathbb{R}^5$$

with constant scalars η_I, $I = 1,2$, and the generalized rotational coordinate $\theta^{(R_3)} \in \mathbb{R}$. Another revolute joint (R_1) is used to fix the first rigid body, representing the collarbone, in the inertial frame. This joint restricts the motion of the collarbone to rotations $\theta^{(R_1)} \in \mathbb{R}$ around the n-axis representing rotations of the torso and leads to five constraints on the first joint (R_1) as

$$g^{(R_1)}(q) = \begin{pmatrix} \varphi^1 - \rho^{11} \\ n^T \cdot d_I^1 - \eta_I, I = 1,2 \end{pmatrix} = 0 \in \mathbb{R}^5,$$

where the reference frame is fixed in the joint (R_1). This selection of the different joints, leading to a system with five degrees of freedom, is the first multi-body model under consideration and denoted by model $M1$. Due to the fact, that in general a forearm is also able to rotate around its body-fixed longitudinal axis n^1, we consider for a second model $M2$ a joint with two rotational degrees of freedom $\theta^{(H_3)} \in \mathbb{R}^2$ for the elbow. This new hinge joint (H_3) is derived in [18], where we found corresponding expressions for the null space matrix, the reparametrization and the forces. This joint allows both hinge (axis n^2 fixed in upper arm) and axial (axis n^1 fixed in forearm) motion and hence leads to four constraints as

$$g^{(H_3)}(q) = \begin{pmatrix} \varphi^3 - \varphi^2 + \rho^{33} - \rho^{23} \\ (n^2)^T \cdot d_1^3 - \eta_1 \end{pmatrix} = 0 \in \mathbb{R}^4. \tag{19}$$

Controls

To control the multi-body system, we assume generalized torques $\tau^{(J_i)}$ acting in the joints J_i, $i = 1,2,3$, between the limbs. Here, we assume that all degrees of freedom, i.e. the rotations of the collarbone, the shoulder, and the elbow, are directly steerable.

Table 1. JOINTS, CONTROLS, AND NUMBER OF DEGREES OF FREEDOM (DOF) FOR THE DIFFERENT MODELS.

	joint	control	dof
$M1$	(R_1, S_2, R_3)	$\left(\tau^{(R_1)}, \tau^{(S_2)}, \tau^{(R_3)}\right)$	5
$M2$	(R_1, S_2, H_3)	$\left(\tau^{(R_1)}, \tau^{(S_2)}, \tau^{(H_3)}\right)$	6
$M3$	(R_1, S_2, R_3)	$\left(\tau^{(R_1)}, \tau^{(S_2)}, E\right)$	5

We investigate two different control models: Firstly, we assume that the generalized torques themselves are the control parameters that have to be determined, i.e. $u = (\tau^{(R_1)}, \tau^{(S_2)}, \tau^{(R_3)}) \in \mathbb{R}^5$ for model $M1$ and $u = (\tau^{(R_1)}, \tau^{(S_2)}, \tau^{(H_3)}) \in \mathbb{R}^6$ for model $M2$, respectively. Secondly, we extend model $M1$ by taking muscle forces into account. For the elbow joint (R_3) the generalized control torque $\tau^{(R_3)}$ is replaced by a torque $\tau^{\text{muscle}}(\theta^{(R_3)}, \dot{\theta}^{(R_3)}, E)$ that results from internal muscle forces existing in that joint. As described in detail in the following section, these muscle forces are configuration and velocity dependent and activated via the activation level $E \in \mathbb{R}$ of the nerves, which now plays the role of the control parameter. Thus, for model $M3$ the control parameters are $u = (\tau^{(R_1)}, \tau^{(S_2)}, E) \in \mathbb{R}^5$. In Tab. 1 an overview of the different joints, the controls, and the number of degrees of freedom (dof) of the three models is presented.

MUSCLE MODELING

The pitcher's arm with muscles is an enhancement of our first arm model M_1 with five degrees of freedom, and so far muscles are only modeled in the elbow joint. A simplified muscle model is used, consisting of the three main muscles in the elbow joint (*Musculus biceps brachii, Musculus brachioradialis* and *Musculus triceps brachii*). Each muscle force is dependent on three elements: the activation level E of the nerves, the function F_l dependent on the muscle length and the contraction velocity v_m described by the Hill's function H. By means of a geometry function $G(\beta)$ the inner muscle force

$$f_m = E \cdot F_l(l_m) \cdot H(v_m) \tag{20}$$

can be transformed to the external muscle force F_m as

$$F_m = G(\beta) \cdot f_m, \tag{21}$$

where l_m is the length of each corresponding muscle and β the angle between upper and forearm (cf. Fig 3). The resulting torque

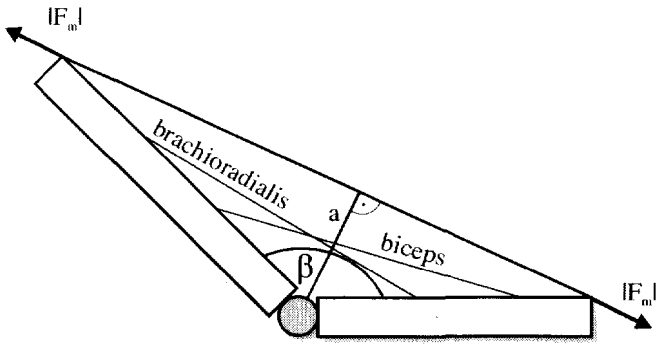

Figure 3. THE ELBOW JOINT WITH MUSCLES (MUSCULUS BRACHIORADIALIS, MUSCULUS BICEPS BRACHII). THE THIRD MUSCLE (MUSCULUS TRICEPS BRACHII) CANNOT BE DESCRIBED GEOMETRICALLY.

that acts in the elbow joint can be determined by

$$\tau^{muscle} = \sum_{k \in M} F_{m_k} \cdot a = \sum_{k \in M} G_k(\beta) \cdot f_{m_k} \cdot a, \tag{22}$$

where the parameter a is generated as shown in Fig. 3 and the functions F_{m_k}, G_k and f_{m_k} have to be established for every muscle $k \in M = \{\text{biceps brachii, brachioradialis, triceps brachii}\}$. Diverse models of muscles can be found in literature and here the work of [13, 17, 19, 20] is applied to construct a model with all desired properties described in detail in [18].

Activation Level

We choose the activation level $E \in [0,1]$ as the control parameter for the force in the elbow joint as described in [21]. While for $E = 0$ the inner muscle forces are zero, maximal magnitudes of the forces are available for an activation level of $E = 1$.

Force-Length Relation

The maximal force that can be generated by the muscle is dependent on its length. Dependent on the numbers of overlapping filaments, the maximal producible force is obtained for a medium muscle length $l_{\max}$ and decreases for a length smaller or bigger than $l_{\max}$. While the qualitative behavior is the same for all muscles, the position of the maximum is individual for each muscle. Thus, the region in which the muscle works differs for different muscles. For the detailed formulas see [17].

Hill's Function

A common model for the dependency of the muscle force on the velocity is the Hill force-velocity relation (see [15]). A function $H(v_m)$ is suggested, that is defined for the concentric part and the excentric part, i.e. if the contraction velocity v_m is positive or negative. For the detailed formulas see again [17].

Geometry Function

The geometry function establishes the connection between the force f_m of a muscle inside the human body and the measurable force F_m outside the body according to the relation

$$F_M = G(\beta) \cdot f_m. \tag{23}$$

Such geometry functions normally have a joint- and muscle specific structure. Approximately, they can be modeled using a substitute muscle such that the resulting geometry function can be used for different joints and muscles, whereas only some muscle specific parameters have to be determined individually, e.g. we use two different geometry functions for the bending and the stretching muscles, respectively.

OPTIMIZATION AND CONSTRAINTS

The aim of the optimization of the pitcher's arm movement is to maximize the velocity of the forearm's center of mass in pitch direction. Consider $d \in \mathbb{R}^3$ as the desired pitch direction, then the discrete objective function to minimize is determined through

$$J(q) = \left\langle \frac{\varphi_N^3 - \varphi_{N-1}^3}{h}, -d \right\rangle, \tag{24}$$

where $\varphi_N^3, \varphi_{N-1}^3$ are the configuration variables of the forearm's center of mass at time $N-1$ and N, respectively and $< \cdot, \cdot >$ describes the standard scalar product.

The pitcher is assumed to begin the motion with prescribed initial configuration and zero velocity. Rather than prescribing final configurations for all present bodies, we prescribe a goal plane for the final position of the hand, where the hand is assumed to be located at the endpoint of the forearm. With e_2 being the pitch direction, the goal plane is formulated as

$$\begin{aligned}\mathcal{M} = \Big\{ & q \in \mathbb{R}^{36} \text{ with} \\ & -\sin\frac{\pi}{4}(l_1+l_2+l_3) \le x^{\text{hand}} \le \sin\frac{\pi}{4}(l_1+l_2+l_3), \\ & (l_2+l_3)\cos\frac{3\pi}{8} \le y^{\text{hand}} \le (l_1+l_2+l_3), \\ & 0 \le z^{\text{hand}} \le \sin\frac{3\pi}{8}(l_1+l_2+l_3) \Big\},\end{aligned}$$

where $(x^{\text{hand}}, y^{\text{hand}}, z^{\text{hand}}) = \varphi^{\text{hand}} = \varphi^3 - \rho^{33} \in \mathbb{R}^3$ is the position of the hand and l_1, l_2, l_3 are the lengths of the first, second, and third body, respectively. During the optimization, the final time T is free but constrained to be in the interval $[0.25, 0.75]$ s, i.e. also the optimal duration of the pitch is determined. In the optimization algorithm this is realized by a variable step size as $h = \lambda \frac{T}{N}$, where $\lambda \in \mathbb{R}$ is an additional optimization variable.

Due to the human body's anatomy, the relative motion in each joint is limited. To obtain a realistic motion, each generalized configuration variable is bounded, for example the forearm is assumed to bend in only one direction. For model $M1$ and $M2$, where the generalized torques themselves are the controls, the incorporation of bounds on the torques is needed since the muscles are not able to create an arbitrary amount of strength. For the implementation we restrict all generalized torques to be within the interval of $[-50, 50]$ Nm. Of course, in reality different muscles groups and limb positions lead to different values for minimal and maximal possible forces in the joints. However, due to the problem of measuring these magnitudes, more sophisticated bounds are difficult to find without taking any muscle model into account. On the contrary, the maximal positive and negative torque in the elbow for the model $M3$ are determined by evaluating τ^{muscle} at the maximal activation level of the muscles $E = 1$. Thus, rather than by constant bounds, the elbow torque is constrained by a function dependent on the angle $\theta^{(R_3)}$ between upper arm and forearm and its velocity $\dot{\theta}^{(R_3)}$ (cf. Fig. 5).

RESULTS

For the optimization of a pitch we need an initial guess of the movement to start with. Through variation and interpolation of four simplified pitch sequences we generate approximately 200 initial guesses for each model. These initial guesses differ additionally in the number of discretization points (nodes). The minimal number of nodes we consider is $N = 10$ and the maximal number is $N = 30$. To solve the resulting constrained optimization problem, we use a sparse SQP optimization algorithm based on SNOPT (see [10] for details) that is implemented in the routine `nag_opt_nlp_sparse` of the NAG library[1]. This algorithm yields different movements as optimal solutions, which are only locally optimal dependent on the initial guess. Due to the strongly nonlinear system, not all initial guesses converge to an optimal solution. In particular, the formulation of the torque τ^{muscle} as given in Eqn. (22) leads to less converged solutions for model $M3$. For the analysis, we consider only those movements, which correspond to converged optimal solutions.

One main observation is, that all three models achieve the same three basic types of pitch movements (cf. Fig. 4). The first movement can be identified by its long outstretched arm movement during the pitch (Fig. 4a). The second movement is executed similar to the first movement, but during the swing back motion the arm is bent (Fig. 4b). The third movement differs significantly from the previous two. Here, the arm is guided above the pitcher's head during the entire movement (Fig. 4c).

[1] `www.nag.com`

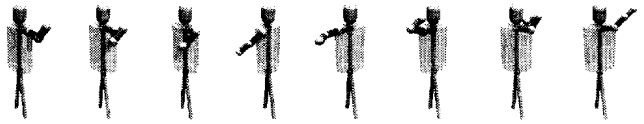

a) Movement 1 is characterized by an outstretched arm.

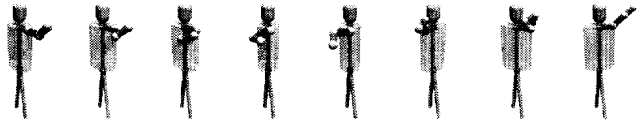

b) Movement 2 is characterized by a bended arm.

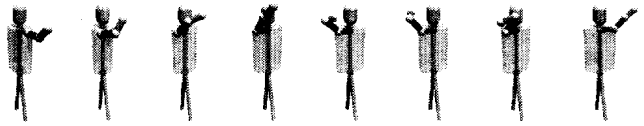

c) Movement 3 is characterized by a motion above the head.

Figure 4. FOR THE OPTIMIZATION INITIATED WITH DIFFERENT INITIAL GUESSES THREE BASIC TYPES OF LOCAL OPTIMAL PITCH MOVEMENTS COULD BE IDENTIFIED FOR ALL THREE MODELS.

Analysis

In Tab. 2 we compare the objective function values[2] and the pitch times for all three movements resulting from the use of the different models $M1$, $M2$ and $M3$. These are averaged values of all converged optimal solutions we obtained by applying the optimization algorithm with the different initial guesses.

Analysis of the Movements For the first analysis of the three movements we compare the particular objective function values. The movement 1 has the largest objective function value, i.e. the highest final velocity of the forearm, followed by movement 2 and movement 3 with the smallest objective function value. This indicates that the movement with the outstretched arm produces most kinetic energy, such that the final velocity of the arm is quite high while movement 3 with a shorter swing back motion leads to a smaller final velocity.

Since the optimal pitch time varies, we can also analyze the final duration time $T \in [0.25, 0.75]$ s of the optimized pitches. For a small step size h, the objective function value J in Eqn. (24) is small, i.e. the final pitch velocitiy is high. Thus, overall in our simulations the time T is near to the minimal time of 0.25 s. Accordingly, a fast pitch implicates a higher velocity compared to a slow pitch. Nevertheless we observe, that movement 1 has the longest duration time with approximately 0.367 s due to the longer swing back motion.

[2] In the following we will identify the objective function value with the velocity of the forearm's center of mass in pitch direction, i.e. the negative value of J defined in Eqn. (24).

Table 2. COMPARISON OF THE OBJECTIVE FUNCTION VALUES AND THE DURATION TIMES BETWEEN THE THREE MODELS.

	movement 1	movement 2	movement 3
$M1$	$30.24\frac{m}{s}$	$25.27\frac{m}{s}$	$24.12\frac{m}{s}$
$M2$	$28.29\frac{m}{s}$	$26.41\frac{m}{s}$	$25.79\frac{m}{s}$
$M3$	$28.5\frac{m}{s}$	$26.32\frac{m}{s}$	$25.79\frac{m}{s}$
time	0.367 s	0.282 s	0.261 s

Analysis of the Models By analyzing the objective function value for each model (cf. Tab. 2), we notice that comparable results are achieved. While for movement 1 the use of M_2 leads to a smaller velocity than M_1, we obtain higher velocities for movements 2 and 3. Indeed, the additional degree of freedom in $M2$ makes the model more realistic and during the movements we observe rotations of the forearm around its longitudinal axis. However, the additional rotational torque provides no contribution to the translatorial velocity of the forearm. Thus, it does not effect the objective function value, whereas for the use of other objective functions, e.g. the control effort, the influence of the new joint would be more significant.

A comparison of $M1$ and $M3$ also shows similar values for both models. That is an expectable result, because the muscle model in $M3$ provides no additional degree of freedom compared to $M1$.

Analysis of the Torques While the control torques for model M_1 and M_2 are restricted by constant lower and upper bounds, the effective muscle torque in model M_3 is restricted by the function given in Eqn. (22). Additionally, this torque is controlled by the activation level of the muscle E. To identify the region of the admissible torque we have to determine the maximal and minimal possible torque in every state of the arm movement. The maximal torque magnitude in the joint with muscles can be achieved with an activation level $E = 1$ while the minimal magnitude of 0 is reached with an activation level $E = 0$. To determine the maximal positive and negative value, we take the sign of the torque into account. Stretching the arm leads to a positive torque while bending results in a negative torque. Thus, the upper bound (dotted line) in Fig. 5 corresponds to the maximal producible torque to induce a stretch motion. On the contrary, the maximal producible torque for the bending motion is represented by the lower bound (dotted line). The area between upper and lower bound corresponds to the admissible region for the torque in the elbow joint. For example, the narrow bounds on the torque in the time intervals $[0.065, 0.098]$ s and $[0.195, 0.24]$ s can be ex-

plained by considering the time evolution of the angle in the elbow joint (cf. solid line in Fig. 5, second diagram), where 0 deg corresponds to a complete bending, 180 deg to an outstretched forearm. Here, the forearm is almost completly bent such that no large torque can be produced resulting from the force-length relation of the muscle. Considering these evolutions, it becomes obvious, that constraining the torque constantly to the interval $[-50, 50]$ Nm is not reasonable.

Due to the choice of the objective function in Eqn. (24), for all three models the optimal control torques in the joints reach the lower and upper bounds several times during the motion as shown for the elbow torque in Fig. 5 (dashed-dotted line: torque produced in the elbow joint without muscles reaches constant bounds given by ± 50 Nm; solid line: torque produced in the elbow joint with muscles reaches bounds given by dotted lines). Thus, to accomplish the optimal pitch movement, maximal producible torques have to be applied.

To analyze the control effort we compute the discrete control effort as

$$||\tau|| = \sum_{k=0}^{N-1} |\tau_k| \cdot h, \tag{25}$$

where $|\cdot|$ is the 1-norm and τ_k is a vector that consists of all torques acting in the joints in the time interval $[t_k, t_{k+1}]$. While motions based on the model $M2$ require the highest control effort resulting from the additionally produced torque and rotation in the hinge joint, the control efforts based on M_1 and M_3 are comparable: Despite different admissible regions for the elbow torque with and without muscles, the produced torque by the muscles leaves the constant region of $[-50, 50]$ Nm only slightly. In some parts of the movement the maximal torque exceeds the constant bounds of $[-50, 50]$ Nm and in some parts it is significantly lower than this constant boundary. According to the results of the final velocity of the three different movements the control effort behaves in a similar way. Movement 1 requires the highest control effort, followed by movement 2 and 3. Thus, movement 1 is the most exhausting pitch movement.

CONCLUSIONS AND FUTURE WORK

Conclusions

In this work, we sucessfully applied a recently developed optimal control method for constrained mechancial systems (DMOCC) to the optimization of a pitch. Three different multibody systems for a pitcher's arm have been modeled and investigated characterized by different joint couplings and controls. In particular, for one model we described the muscle interaction by using a muscle function consisting of three main muscles in the elbow. A comparison of the optimal movements as well as

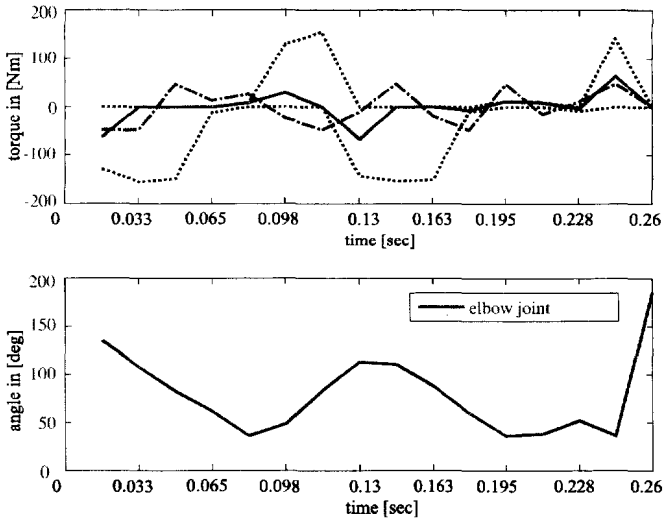

Figure 5. COMPARISON OF THE EFFECTIVE TORQUE AND THE ANGLE IN THE ELBOW JOINT (BOTTOM) FOR MOVEMENT 3. TOP: TORQUES GENERATED BY THE MUSCLE FORCE (DASHED-DOTTED LINE: JOINT WITHOUT MUSCLES; SOLID LINE: JOINT WITH MUSCLES; DOTTED LINE: BOUNDS FOR MUSCLE MODEL).

a comparison of the different multi-body models lead to the following main observations: Firstly, all three models achieve the same three basic types of optimal pitch movements (cf. Fig. 4) resulting form the use of different initial guesses, whereas a swing back motion with a long outstrechted arm provides the highest final pitch velocities. Secondly, an additional applied torque in the elbow (by using a hinge joint rather than a revolute joint) allows rotation of the forearm around its longitudinal axis but does not lead to a higher final velocity. Of course, in general it is desirable to consider a most realistic model as possible. However, to decrease the complexity of the problem, the use of a simplified model might be sufficient dependent on the specific task defined by the objective function. Thirdly, the use of a muscle model automatically constrains the maximal producible torque in the elbow joint dependent on the angle position and the angle velocity in the elbow. This leads on the one hand to more realistic bounds on the applied external torques and on the other hand to more insight into the optimal time evolution of the muscle forces acting in the joints. Although the muscle model increases the complexity of the problem it is an enrichment and should be taken into account especially for biomechanical applications.

Future Work

Although only a simplified model is used, the optimal motions of the kinematic chain can already be identified with realistic pitch motions in a reasonable way. However, as for the bounds on the torques resulting from a muscle function, it would be desirable to obtain more sophisticated bounds on the config-

uration variables as well as including constraints to avoid intersections between the bodies in the chain. Since usually not only one objective is of interest, different objective functions have to be considered and the solutions should be compared. In addition, a model of the full human body equipped with more muscles is desirable to take the effects of other limbs into account. Especially in the area of sport motions, optimal results are usually dependent on the behavior of the entire body. The knowledge gained from optimal control simulations might help to improve individual techniques or even leads to the development of new techniques (as it could be observed during the last decays, e.g. for high- and ski jumping).

ACKNOWLEDGMENTS

Thanks go to Helmut Böhmer and Sigrid Leyendecker for helpful discussions. This research was partly supported by the AFOSR grant FA9550-08-1-0173.

REFERENCES

[1] Leyendecker, S., Ober-Blöbaum, S., Marsden, J. E., and Ortiz, M., 2008. Discrete mechanics and optimal control for constrained systems (DMOCC). Submitted to *Optimal Control, Applications and Methods.*

[2] Ober-Blöbaum, S., 2008. "Discrete mechanics and optimal control". PhD thesis, University of Paderborn.

[3] Ober-Blöbaum, S., Junge, O., and Marsden, J. E., 2008. Discrete mechanics and optimal control – an analysis. Submitted to *ESAIM: Control, Optimisation and Calculus of Variations.*

[4] von Stryk, O., 1993. "Numerical solution of optimal control problems by direct collocation". In *Optimal Control - Calculus of Variation, Optimal Control Theory and Numerical Methods*, R. Bulirsch, A. Miele, J. Stoer, and K. H. Well, eds., Vol. 111 of *International Series of Numerical Mathematics*. Birkhäuser, pp. 129–143.

[5] Bock, H. G., and Plitt, K. J., 1984. "A multiple shooting algorithm for direct solution of optimal control problems". In 9th IFAC World Congress, Pergamon Press, pp. 242–247.

[6] Betts, J. T., 1998. "Survey of numerical methods for trajectory optimization". *AIAA J. Guidance, Control, and Dynamics,* **21**(2), pp. 193–207.

[7] Betts, J. T., 2001. "Practical methods for optimal control using nonlinear programming". *SIAM, Philadelphia, PA.*

[8] Marsden, J. E., and West, M., 2001. "Discrete mechanics and variational integrators". *Acta Numerica,* **10**, pp. 357–514.

[9] Barclay, A., Gill, P. E., and Rosen, J. B., 1998. "SQP methods and their application to numerical optimal control". In Variational Calculus. Optimal Control and Application, W. H. Schmidt, K. Heier, L. Bittner, and R. Bulirsch, eds.

[10] Gill, P. E., Murray, W., and Saunders, M. A., 1997. SNOPT: An SQP algorithm for large-scale constrained optimization. Report NA 97-2, Department of Mathematics, University of California, San Diego, CA, USA.

[11] Leyendecker, S., Ober-Blöbaum, S., Marsden, J. E., and Ortiz, M., 2007. "Discrete mechanics and optimal control for constrained multibody dynamics.". In 6th International Conference on Multibody Systems, Nonlinear Dynamics, and Control, ASME International Design Engineering Technical Conferences.

[12] Betsch, B., and Leyendecker, S., 2006. "The discrete null space method for the energy consistent integration of constrained mechanical systems. Part II: Multibody dynamics". *International Journal for Numerical Methods in Engineering,* **4**, pp. 499–552.

[13] Sust, M., 1996. "Modular aufgebaute deterministische Modelle zur Beschreibung menschlicher Bewegung". In Grundlagen der Biomechanik des Sports, R. Ballreich and W. Baumann, eds., Ferdinand-Enke-Verlag.

[14] Murray, W., Buchanan, T., and Scott, D., 2000. "The isometric functional capacity of muscles that cross the elbow". *Journal of Biomechanics,* **33**, pp. 943 – 952.

[15] Hill, A., 1938. "The heat of shortening and the dynamic constants of muscle". *Proceedings of the Royal Society,* **126**, pp. 136– 195.

[16] Gerbaux, M., Turpin, E., and Lensel-Corbeil, G., 1996. "Musculo-articular modelling of the triceps brachii". *Journal of Biomechanics,* **29**, pp. 171–180.

[17] Giesl, P., Meisel, D., Scheurle, J., and Wagner, H., 2003. Stability analysis of the elbow with a load.

[18] Timmermann, J., 2008. Die Nullraum-Methode in Kombination mit DMOC zur optimalen Steuerung mechanischer Systeme mit holonomen Zwangsbedingungen. Diploma thesis, University of Paderborn.

[19] Wagner, H., Machalett, M., and Blickhan, R., 2003. "Bewegungslernen und Attraktorstabilität - Vorläufige Ergebnisse und Anwendungen". In Biomechanik als Anwendungsforschung - Transfer zwischen Theorie und Praxis, H. Riehle, ed., Vol. 132, Czwalina Verlag.

[20] Spägele, T., 1998. "Modellierung, Simulation und Optimierung menschlicher Bewegungen". PhD thesis, Institut A für Mechnik der Universität Stuttgart.

[21] Stelzer, M., and von Stryk, O., 2008. "Walking, running and kicking of humanoid robots and humans". In From Nano to Space, Breitner, Denk, and Rentrop, eds., Springer Verlag, pp. 175–192. Preprint.